JOURNAL OF GEOPHYSICAL RESEARCH, VOL. 111, D18307, doi:10.1029/2006JD007298, 2006

Critique of the tracer-tracer correlation technique and its potential to analyze polar ozone loss in chemistry-climate models

Carsten Lemmen,[1,2] Rolf Müller,[1] Paul Konopka,[1] and Martin Dameris[3]

Received 14 March 2006; revised 15 May 2006; accepted 30 June 2006; published 29 September 2006.

[1] The tracer-tracer correlation technique (TRAC) has been widely employed to infer chemical ozone loss from observations. Yet, its applicability to chemistry-climate model (CCM) data is disputed. Here, we report the successful application of TRAC on the results of a CCM simulation. By comparing TRAC-calculated ozone loss to ozone loss derived with the passive ozone method in a chemistry transport model we differentiate effects of internal mixing and cross vortex boundary mixing on a TRAC reference correlation. As a test case, we consider results of a cold Arctic winter/spring episode from an E39/C experiment, where typical features, for example, sufficient polar stratospheric cloud formation potential, denitrification and dehydration, and intermittent and final stratospheric warming events, are simulated. We find that internal mixing does not impact the TRAC-derived reference correlation at all. Mixing across the vortex boundary would lead to an underestimation of ozone loss by ~10% when calculated with TRAC. We provide arguments that TRAC is a consistent and conservative method to derive chemical ozone loss and can be used to extract its chemical signature also from CCM simulations. As a consequence, we will be able to provide a lower bound for chemical ozone loss for model simulations where a passive ozone tracer is not available.

Citation: Lemmen, C., R. Müller, P. Konopka, and M. Dameris (2006), Critique of the tracer-tracer correlation technique and its potential to analyze polar ozone loss in chemistry-climate models, *J. Geophys. Res.*, *111*, D18307, doi:10.1029/2006JD007298.

1. Introduction

[2] In the most recent *World Meteorological Organization* (*WMO*) [2003] ozone assessment, predictions from chemistry-climate models (CCM) for the evolution of the past and future Arctic polar ozone layer were presented based on the CCM intercomparison study by *Austin et al.* [2003]. As a measure of the skill of CCMs in reproducing polar O_3 loss, the minimum springtime O_3 column was introduced, which allows for comparison amongst a variety of CCMs with TOMS observations and with results presented in the former *WMO* [1999] assessment. Averaged over all models (UMETRAC [*Austin*, 2002], CCSR [*Nagashima et al.*, 2002], CMAM [*de Grandpré et al.*, 2000], MAECHAM/CHEM [*Steil et al.*, 2003], and E39/C [*Hein et al.*, 2001; *Schnadt et al.*, 2002]) a significant negative trend in minimum column O_3 (−17 Dobson units (DU) per decade) was seen in the period 1979 to 2000 in close agreement with observations. *Austin et al.* [2003] placed the start of O_3 recovery in the period 2000–2020, based in part on time slice simulations with E39/C (years 1990 and 2015 boundary conditions), CMAM (2000 and 2030), and MAECHAM/CHEM (2000 and 2035). The predictive power of these CCM simulations for the Arctic was questioned by the latest *Intergovernmental Panel on Climate Change/Technology and Economic Assessment Panel* [2005] assessment due to large model uncertainties or deficiencies: further model development and validation is called for.

[3] On the basis of minimum column O_3 one cannot distinguish between dynamical processes that influence the O_3 column and changes in the chemical regime. For example, *Schnadt and Dameris* [2003] found an increase of minimum column O_3 from 1990 to 2015 in E39/C simulations. This apparent recovery, however, can be attributed to enhanced planetary wave activity which results in higher stratospheric temperatures. In fact, for their "1990" experiment, *Schnadt* [2001] and *Schnadt et al.* [2002] calculated only weak chemical O_3 loss in the time slice average using daily simulated O_3 loss rates. While the minimum springtime O_3 column is a readily available quantity in CCMs and can be compared amongst different numerical models, a quantification of chemical O_3 loss is neither routinely performed, nor is there an easily comparable or well established measure of chemical O_3 loss in CCM simulations. To make judgments about the effect of chlorofluorocarbon (CFC) changes on the ozone layer,

[1]Institut für Chemie und Dynamik der Geosphäre I: Stratosphäre, Forschungszentrum Jülich GmbH, Jülich, Germany.

[2]Now at Copernicus Instituut voor Duurzame Ontwikkeling en Innovatie, Sectie Natuurwetenschappen en Samenleving, Universiteit Utrecht, Utrecht, Netherlands, and Institut für Küstenforschung, GKSS-Forschungszentrum Geesthacht GmbH, Geesthacht, Germany.

[3]Institut für Physik der Atmosphäre, Deutsches Zentrum für Luft- und Raumfahrt e.V., Oberpfaffenhofen, Wessling, Germany.

0148-0227/06/2006JD007298$09.00

however, it is the change in chemical O_3 loss that needs to be assessed.

[4] For deducing chemical O_3 loss from observations, a variety of methods has been employed to Arctic late winter/spring episodes since the early nineties. *WMO* [2003] discriminates methods to quantify chemical O_3 loss into one group which uses explicit transport calculations and another group, where effects of transport are implicitly accounted for. In the first group, observations from a variety of platforms, e.g., ozonesondes, satellites, balloons, are connected in time and space by considering vortex average descent [e.g., *Knudsen et al.*, 1998; *Rex et al.*, 2004], transport model calculations [e.g., *Goutail et al.*, 2005], or ensembles of Lagrangian trajectories [e.g., *Manney et al.*, 1997]. Furthermore, the 'Match' technique has been employed which makes use of a statistical analysis of subsequent ozonesonde measurements along calculated trajectories [*von der Gathen et al.*, 1995; *Rex et al.*, 2002]. O_3 loss is determined with respect to a prior measurement of ozone (O_3^{start}).

[5] Implicit consideration of transport is provided by observing changes in the relation between O_3 and a long-lived tracer (tracer-tracer correlation, TRAC [*Proffitt et al.*, 1990; *Tilmes et al.*, 2004]). While relations between H_2O and O_3 were already published by *Roach* [1962], *Proffitt et al.* [1990] first used the change in the relation between N_2O and O_3 to infer chemical O_3 loss. Subsequently, concurrent measurements of O_3 and a passive tracer like HF or CH_4 derived from the Halogen Occultation Experiment (HALOE) instrument were used to estimate chemical O_3 losses during 1990s winters [e.g., *Müller et al.*, 1997] and during the last decade [*Tilmes et al.*, 2004]. Furthermore, the TRAC technique was used to quantify chemical O_3 losses derived from observations by the ILAS II satellite [*Tilmes et al.*, 2006], balloon-borne instruments [*Müller et al.*, 2001; *Salawitch et al.*, 2002], and high-altitude aircraft [*Richard et al.*, 2001; *Ulanovskii et al.*, 2004]. Using HALOE and ER2 observations of the correlation between CH_4 and O_3, *Fairlie et al.* [1999] validated their mixing algorithm to predict chemical ozone loss during the POLARIS campaign in summer 1997.

[6] While TRAC has been applied extensively to observational data, the potential of TRAC for simulated data sets has not been exploited due to lack of need and arguments discouraging its use. In chemistry transport models (CTMs), the simultaneous simulation of a chemically inert O_3 tracer (passive ozone, O_3^{pass}) gives a reliable measure of chemical O_3 loss [e.g., *Lefèvre et al.*, 1998; *Sinnhuber et al.*, 2000; *Konopka et al.*, 2004], obliterating the need for a correlation-based analysis of chemical O_3 loss. For their CCM CMAM, *Sankey and Shepherd* [2003] deny applicability of TRAC: neither do their simulations exhibit a compact tracer-O_3 relationship nor is the polar vortex sufficiently isolated. This finding leads *Sankey and Shepherd* [2003] to suggest that TRAC may not be applicable to model data in general.

[7] Here, we demonstrate for simulated data obtained with the CCM E39/C [*Hein et al.*, 2001] that TRAC can be used for the calculation of chemical O_3 loss. We corroborate earlier findings [e.g., *Müller et al.*, 2001; *Rex et al.*, 2002; *Konopka et al.*, 2004] that application of TRAC will underestimate O_3 loss and is thus a conservative measure of O_3 loss. Like for observations, for model data the establishment of a compact early vortex relationship and a sufficient isolation of the vortex are required to ensure applicability of the technique. High numerical diffusion complicates the TRAC analysis of simulated data. We demonstrate how the validity of TRAC can be tested by employing computationally inexpensive trajectory calculations and show that vortex strength and a compact relationship can be found for the E39/C simulation. By analogy with a Lagrangian simulation with strongly enhanced mixing, we deduce the magnitude of the impact of E39/C numerical diffusion on TRAC. The possibility of using TRAC on CCM data for the analysis of chemical O_3 loss should contribute to ongoing initiatives for process-oriented validation of CCMs [*Eyring et al.*, 2005].

2. Tracer-Tracer Relations

[8] The tracer-tracer correlation technique (TRAC) relates two tracers with different physicochemical life times within the vortex to one another [*Proffitt et al.*, 1990]. For seasonal studies like those of polar O_3 loss or polar winter denitrification, CH_4, N_2O, or HF were used as long-lived tracers. The short-lived compounds considered are O_3 (chemically altered by a variety of catalytic cycles), HCl (reservoir converted to active chlorine), or total active nitrogen (NO_y, removed from an air mass by particle sedimentation) [e.g., *Fahey et al.*, 1989; *Proffitt et al.*, 1990; *Müller et al.*, 1996; *Rex et al.*, 1999; *Tilmes et al.*, 2004].

[9] Within an isolated air mass, any tracer-tracer relationship will remain unaltered if physicochemical processes are absent, even though the air mass undergoes advection and deformation. Therefore, in the absence of mixing, a change in the relationship quantifies the effect of the respective physicochemical process under consideration [e.g., *Salawitch et al.*, 2002; *Tilmes et al.*, 2004; *Müller et al.*, 2005]. The change of the relationship between two tracers can be evaluated quantitatively only if the early winter correlation is sufficiently compact: Compact relationships evolve when the horizontal mixing timescale is shorter than the chemical life time within an enclosed region. Larger-scale isentropic mixing following differential descent may contribute to a linearization and compactization of a curved tracer-tracer relationship [e.g., *Michelsen et al.*, 1998, Plate 2]; on the other hand, singular vertical mixing events may produce outliers. A compact relationship is best established after the formation and isolation of the polar winter vortex and before photochemical O_3 loss sets in; for the Arctic region, late December or early January measurements are suggested by *WMO* [2003]. Compact vortex relationships are evident in an accumulation of tracer-tracer values around a unique reference relation in the vortex; this early winter relationship can be used as a reference for subsequent physicochemical changes. Outside the polar vortex, the photochemical life time of O_3 is shorter than inside, resulting in a noncompact relationship [*Plumb and Ko*, 1992; *Proffitt et al.*, 1992]. The subtropical relationship is approximated by a straight line determined by increasing photochemical destruction of CH_4 and production of O_3 with altitude. When the polar vortex breaks up in spring, the two distinct relationships merge [*Morgenstern et al.*, 2003].

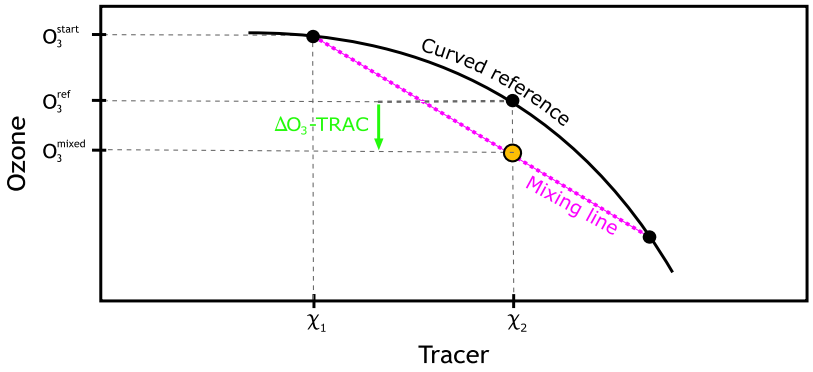

Figure 1. Sketch of the impact of internal mixing on ozone loss calculations which use a reference relationship (O_3^{ref}). The situation shown is strongly exaggerated and applies if mixing (along dotted line with result shown as open circle) occurs after differential descent between air parcels widely separated on a convex relationship.

[10] Even if a compact relationship can be found, mixing of air masses that are separated in tracer space can impact the applicability of TRAC, i.e., (1) internal mixing or (2) mixing across the vortex boundary. Internal mixing, also referred to as anomalous mixing [*Plumb et al.*, 2000], may lead to errors in a TRAC-like analysis if the compact relationship is curved as is, for example, the case for the vortex relation between N_2O and NO_y [*Esler and Waugh*, 2002]. If mixing between two air parcels (APs) with very different N_2O mixing ratios (corresponding to different altitudes) occurs, the resultant mixed AP configuration lies on a mixing line connecting the two originating AP positions in tracer space below the reference relation, leading to an overestimation of denitrification by TRAC. On the other hand, mixing between air masses with very different tracer-tracer relations, in particular between the vortex and midlatitude relationship, can lead to underestimation with TRAC: Intensive investigations by, e.g., *Müller et al.* [2001], *Tilmes et al.* [2004], or *Müller et al.* [2005], consistently found that if mixing with extravortex air occurred, this would tend to increase ozone at a given tracer level and would therefore lead to an underestimation of O_3 loss calculations with TRAC.

[11] Empirical results for the impact of internal and cross vortex mixing were published by, e.g., *Richard et al.* [2001], *Ray et al.* [2002], *Salawitch et al.* [2002], and *Konopka et al.* [2004] for the Arctic winter 1999/2000. On the basis of a N_2O-O_3 relation from in situ observations, the chemical O_3 loss calculated by *Salawitch et al.* [2002] is not significantly influenced by either internal nor cross vortex mixing. *Richard et al.* [2001] used the curved N_2O-CO_2 relation to demonstrate that internal mixing did not affect calculated ΔO_3 and showed, by using CFC-11 observations, that entrainment of midlatitude air into the vortex was not significant. *Ray et al.* [2002] examined the influence of differential descent on tracer-tracer correlations using five tracers with different photochemical life time and found that the majority of differential descent and subsequent homogenization took place in early winter. Compared to O_3 loss calculated with a passive O_3 tracer, *Konopka et al.* [2004] found that mixing of polar vortex with midlatitude air decreased chemical O_3 loss calculated with a CH_4-O_3 correlation by 100–400 ppbv. They also showed that only unrealistically exaggerated vertical mixing would lead to an overestimation of O_3 loss by TRAC.

2.1. Internal Mixing

[12] Within the polar vortex, differential descent may arise from slowly adjusting low temperatures in the core and strong cooling toward the edge, and may lead to (internal) mixing between APs originating from different altitude levels. The effect of an internal mixing event on tracer-ozone relationships is sketched in Figure 1 [cf. *Ray et al.*, 2002, Figure 6d]: An AP (χ_1, O_3^{start}) on the early winter curved vortex reference relationship (black line) is mixed with an AP on the same reference relationship but separated in tracer space, i.e., following unmixed differential descent. Mixing along a mixing line (blue) results in a mixed AP (χ_2, O_3^{mixed}, solid orange dot) which lies below the reference relation. The mixed AP deviates from the reference relationship the more the stronger the correlation is curved and the wider the originating APs are separated [e.g., *Michelsen et al.*, 1998]. In chemical O_3 loss calculations, this underestimation $\Delta O_3\text{-TRAC} = O_3^{ref} - O_3^{mixed}$ (green arrow in Figure 1) may erroneously be interpreted as additional ozone loss. To circumvent the problematic curvature in tracer-tracer relationships, *Esler and Waugh* [2002] employed an artificial tracer which is constructed from a linear combination of chemical tracers and is a linear function of the long-lived tracer. Suitable tracers to construct a linear relationship are often not available from observations, neither are they available from the data set used for this study.

2.2. Mixing Across the Vortex Edge

[13] In addition to mixing within the vortex, isentropic mixing during the winter and spring occurs across the vortex edge along lines connecting (in tracer-ozone space) the vortex relation with the midlatitude relation [*Plumb et al.*, 2000; *Müller et al.*, 2005]. Mixing across the vortex edge dilutes the vortex air and is often observed as thin filaments of midlatitude air within the vortex. This process is mainly triggered by planetary waves; midlatitude air intrudes into the vortex at locations where the PV gradient at the edge is particularly weak [*Steinhorst et al.*, 2005].

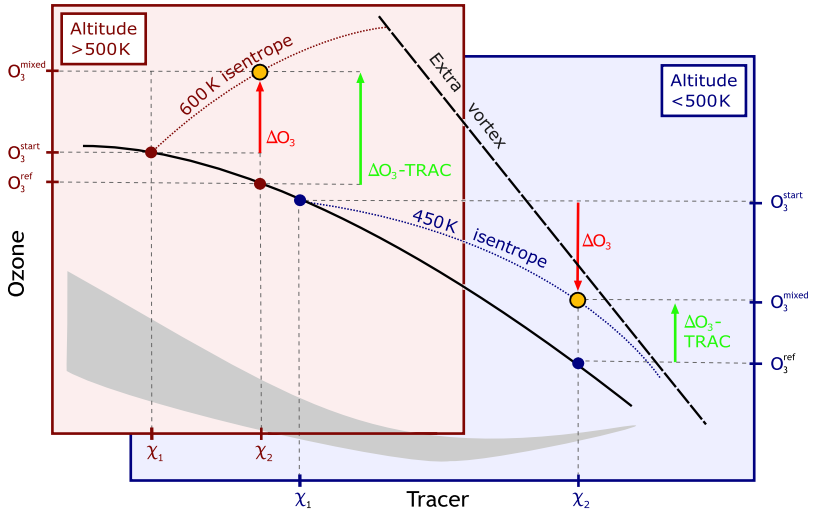

Figure 2. Close-up sketch of the impact of continuous mixing on O_3 loss estimates using either an initial value of O_3 or a reference relationship. Mixing occurs along isentropes (dotted lines) between air parcels on the reference relationship (black solid line) toward the midlatitude relationship (black dashed). At higher altitudes, isentropes are near perpendicular to the reference relation (left, red-shaded). At low altitudes, isentropes are near parallel to the reference relation (right, blue-shaded). For the implications on loss calculations see text.

This (irreversible) transport across the vortex edge dilutes or increases the O_3 mixing ratios within the vortex depending on whether outside vortex O_3 mixing ratios are less than or greater than the inside mixing ratios. For chemically unperturbed conditions, inside vortex O_3 mixing ratios are greater than outside the vortex above ~500 K, and smaller than outside below ~500 K, owing to opposite horizontal gradients building up as the consequence of the diabatic descent of the vortex relative to the surf zone.

[14] To understand how (isentropic) mixing may influence the chemical O_3 loss deduced via the TRAC method (that neglects this effect), we discuss in Figure 2 how such a purely dynamical process can be misinterpreted as chemical loss or as production of O_3. Let us consider an AP within the vortex characterized by a tracer with a mixing ratio χ_1. The corresponding ozone mixing ratio, O_3^{start}, can be derived from the TRAC early vortex correlation (thick solid line) if, according to our previous discussion, a compact tracer-ozone correlation had formed within the well-isolated vortex. The isentropic mixing of such an air mass with midlatitude air occurs along isentropes connecting the TRAC early vortex correlation with the midlatitude correlation (dotted lines). The resulting mixed AP (outlined yellow dots) can be characterized by a tracer mixing ratio χ_2 and an ozone mixing ratio O_3^{mixed}. The ozone change, $\Delta O_3 = O_3^{mixed} - O_3^{start}$ (red arrows) has different signs above (Figure 2, left red-shaded) and below (Figure 2, right blue-shaded) ~500 K. The corresponding ozone change with respect to the TRAC early vortex correlation, i.e., with respect to O_3^{ref}, are denoted by green arrows. Note that although ΔO_3 changes sign between the two altitude ranges sketched in Figure 2, ΔO_3-TRAC is always positive.

[15] In recent cold polar winters, the spring tracer-ozone correlation within the vortex is strongly affected by chemical O_3 loss [e.g., *Tilmes et al.*, 2004, 2006] and can be found clearly below the early vortex correlation (gray regions). The difference between the early vortex reference and the spring correlation quantifies the chemical O_3 loss [*Michelsen et al.*, 1998]. Whereas mixing above and below ~500 K enhances or dilutes vortex O_3 (opposite signs of the red arrows), this process quantified with respect to the TRAC reference always leads to positive values of ΔO_3 (green arrows, see Appendix A for a detailed explanation). This consistency holds even below 500 K, where the O_3 mixing ratios are reduced by the mixing in of outside vortex air. Using TRAC, correlation values above the reference are interpreted as O_3 production which excludes the possibility that mixing may lead to an overestimation of chemical O_3 loss. Furthermore, the impact of mixing that is shifting upward (along the green arrows) the early vortex correlation toward higher values decreases with altitude because below ~500 K the shape of an isentrope only slightly differs from the TRAC reference curve. O_3 loss in the region below 500 K contributes most to column O_3 loss.

[16] This property makes chemical O_3 loss derived from TRAC rather robust with respect to mixing processes. In contrast to TRAC, all methods that rely solely on O_3 measurements to diagnose polar chemical O_3 loss are less predictably affected by mixing. In particular, as shown in Figure 2 (right), mixing into the vortex below ~500 K dilutes O_3 (negative ΔO_3 along the red arrow) and, consequently, cannot be distinguished from chemical O_3 loss. O_3 loss diagnostics based on O_3 profiles sampled during the winter within the vortex may be systematically biased by accumulated dilution of the vortex and, consequently, may lead to an overestimate of chemical O_3 loss. In Appendix A, we quantify the errors of methods referring either to a starting value of O_3 or to a value on the reference relationship with respect to a passive ozone

tracer. We show that these errors are independent of chemical ozone loss.

3. Models and Data

[17] The Chemical Lagrangian Model of the Stratosphere (CLaMS) is a Lagrangian CTM hierarchy; details of the model are described in *McKenna et al.* [2002a, 2002b]. For passive tracer studies we make use of two core components of CLaMS, these are (1) Lagrangian advection on isentropes and cross-isentropic motion and (2) Lagrangian mixing based on flow deformation [*Konopka et al.*, 2004]. Diabatic displacement is calculated from heating rates obtained from radiative transfer calculations [*Zhong and Haigh*, 1995]. This model constellation was previously used by *Konopka et al.* [2005] to quantify mixing during the unusual Antarctic vortex split in September 2002.

[18] Wind and temperature fields for CTM simulations are provided by a late winter/spring episode from a CCM time slice experiment performed with ECHAM4.DLR(L39)/CHEM (abbreviated E39/C [*Hein et al.*, 2001]). E39/C operates on 39 pressure levels with the upper boundary centered at 10 hPa and high vertical resolution, which is about 700 m near the tropopause [*Land et al.*, 2002]. The adopted horizontal resolution is T30, i.e., dynamical processes have an isotropic resolution of about 670 km. Microphysics and chemistry are calculated on the corresponding Gaussian transform grid with a horizontal resolution of $3.75^\circ \times 3.75^\circ$ latitude by longitude. Model dynamics are interactively coupled to the stratospheric chemistry module CHEM developed by *Steil et al.* [1998]: Advected and chemically altered greenhouse gases feed back onto the radiation scheme and in this way influence model dynamics. E39/C has been found to produce realistic pattern agreement of the geographical distribution of O_3 in comparison with European Centre for Medium-Range Weather Forecasts reanalyses from 1979 to 1994. The O_3 column is globally overestimated by about 10–15% [*Austin et al.*, 2003]. Results derived from time slice experiments with E39/C were used in the recent *WMO* [2003] assessment for both hindcasting and prediction of the spring Arctic minimum O_3 column: These show an increasing O_3 column by 2015 after the decrease from the 1960s and low values in the 1990s. While E39/C predicts a small recovery around 2015, other CCMs (e.g., UMETRAC) place their ozone minimum around this time.

[19] We chose to analyze a cold winter/spring episode from the '2015' experiment [*Schnadt et al.*, 2002], where increased planetary wave activity and associated higher frequency of stratospheric warming events [*Schnadt and Dameris*, 2003] present a good test bed for the validation of TRAC in dynamically active winters. Out of this 20-year ensemble, the 16th cycle exhibits the lowest temperatures and the largest chemical O_3 loss. Daily midnight and noon temperature and wind fields in the archived E39/C data are analyzed for (1) temperatures below the nitric acid trihydrate (NAT) existence temperature (T_{NAT} [*Hanson and Mauersberger*, 1988]); (2) indications of stratospheric warmings as classified by *Labitzke* [1999]; and (3) area within the vortex edge, defined by *Nash et al.* [1996] at the largest potential vorticity-equivalent latitude gradient; equivalent latitude (ϕ_{eq}) is equated to the latitude circle which encompasses the same area as the area enclosed by a given potential vorticity (PV) contour. The employed data cover the period from 1 January to 1 April; from a large area of sub-T_{NAT} temperatures in January and early February (10^6 km^2), three minor warmings successively reduce the polar vortex area on 12 February, 20 February, and 14 March. A major warming on 25 March disturbs the polar vortex; westerly zonal circulation is restored by 30 March (summer circulation sets in after 16 April).

[20] E39/C tracer fields are available in 90-day intervals starting on 1 January. Initial mixing ratios for O_3, CH_4, and N_2O are interpolated from the January E39/C data set onto the CLaMS grid with a mean horizontal AP distance of r = 200 km and distributed vertically in nine major isentropic levels corresponding to an aspect ratio of $\alpha = 250$ [*Konopka et al.*, 2004]. Within each main level APs are permuted vertically onto nine sublevels. Artificial tracers to mark the (fixed) upper and lower model boundary layers are added for diagnostic purposes as is a tracer marking the initial potential temperature (Tr_θ) of each AP. A vortex tracer (Tr_V) is set to one for AP north of the vortex edge (defined below) and to zero elsewhere. Within the CTM, tracers are advected and mixed every 24 hours with the critical flow deformation parameter $\ell_c = 1.2$ [*Konopka et al.*, 2004]. The resultant CLaMS-simulated tracer distribution is used as a reference data set for the E39/C-simulated tracer fields which are interpolated onto the quasi-uniform CLaMS AP positions.

[21] The probability density function of the relation between CH_4 and O_3 in January exhibits two distinct branches which evolved due to the isolation of vortex air masses from midlatitude air (Figure 3). O_3 mixing ratios inside the polar vortex are lower (lower left branch) than subtropical O_3 mixing ratios (upper right branch). The isolation of the vortex air is provided by a dynamical transport barrier which is, e.g., apparent in an intersection of isentropes (on which horizontal transport occurs) with isopleths of PV at large angles [*Steinhorst et al.*, 2005]. In ϕ_{eq}-PV space, the polar vortex edge is evident as the strongest gradient of PV(ϕ_{eq}), located near the location of the strongest zonal wind [*Nash et al.*, 1996]. Following the idea by *Nash et al.* [1996], the vortex edge is determined separately for each potential temperature: A seventh-order polynomial is fitted to the PV(ϕ_{eq}) data. First- to third-order derivatives of these polynomial expressions are evaluated to calculate the inflection point (steepest gradient, vortex boundary) and points of maximum curvature (i.e., surf zone boundary and vortex core boundary) adjacent to the wind maximum. The resulting vortex edge is indicated in Figure 3 as a dashed line.

[22] The compact vortex relationship between January CH_4 and O_3 can be approximated by a functional dependence of O_3 mixing ratio Y on the CH_4 mixing ratio X. To determine this reference relationship and to avoid impact of the upper boundary on the fit, for each isentropic level the median values of CH_4 and O_3 are calculated; a second-order polynomial is determined with a least squares fit to the median values and yields the analytical expression

$$Y = -9.6X^2 + 24.6X - 11.1 \quad (1)$$

in units of parts per million by volume (ppmv). Relationship (1) is shown in Figure 3 as a solid line, it can be used to

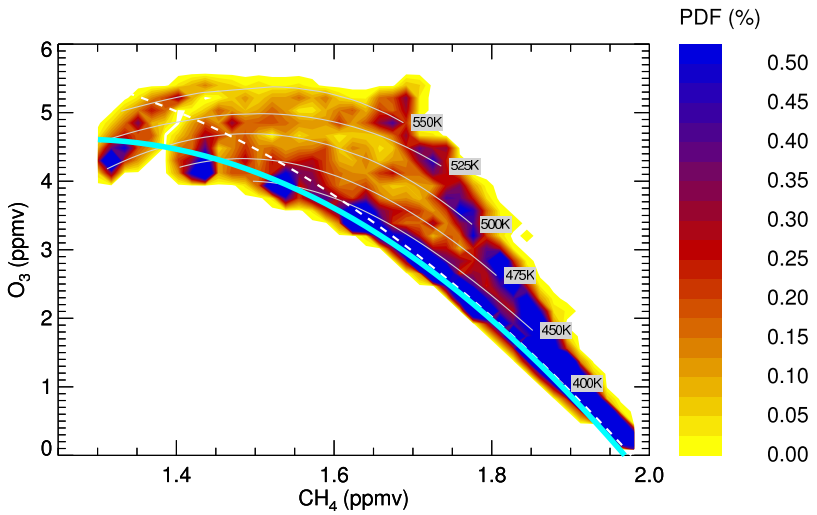

Figure 3. Probability density function of stratospheric O_3 versus CH_4 for January data north of 15°N and between 380 and 550 K potential temperature from E39C. Two distinct branches of the distribution have evolved, one in the polar vortex (below dashed line) and one in the extratropics. The thick solid line shows the early vortex relation given by equation (1); the shape of isentropes is indicated by thin lines.

calculate the O_3 field that would be expected inside the vortex in the absence of chemical change.

4. CLaMS Tracer Simulations

[23] Mixing-induced changes to the tracer-tracer correlation can be identified with the help of a passive ozone tracer (O_3^{pass}). The difference between the O_3 field derived from the reference correlation and O_3^{pass} quantifies those transport effects that are not implicitly accounted for by the TRAC technique, namely internal mixing and cross-vortex boundary mixing. O_3^{pass} is not available in E39/C; we use the CLaMS CTM to simulate advection and mixing of CH_4 and O_3^{pass}, driven by the CCM wind field. Figure 4 shows O_3^{pass} as a function of CH_4 on 1 April, together with the early winter reference relationship (solid line). The CH_4-O_3^{pass} vortex relationship is shown as the dashed line. O_3^{pass} mixing ratios in the vortex are greater than O_3 mixing ratios

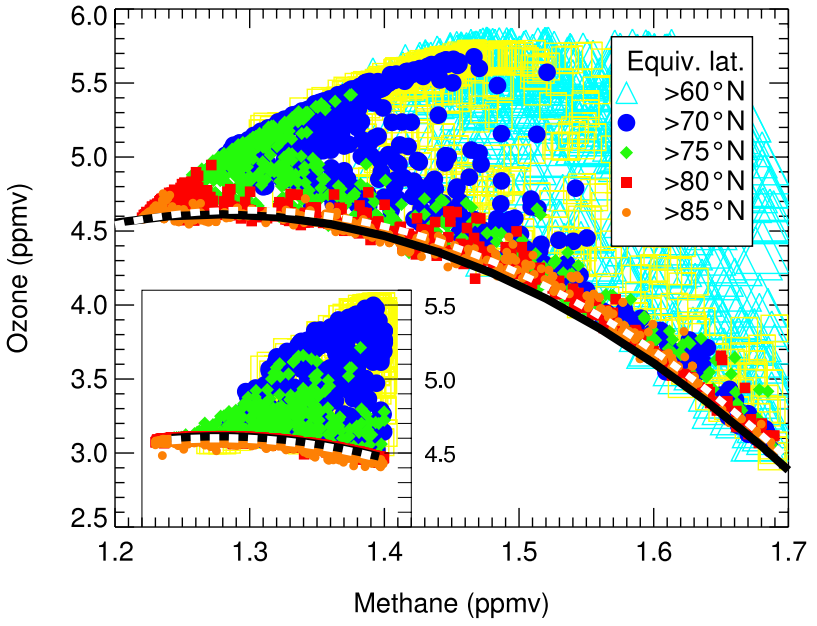

Figure 4. CLaMS spring distribution of APs in CH_4-O_3 space, resolved by equivalent latitude. Because of mixing, O_3^{pass} within the remaining vortex ($\phi_{eq} > 80°N$, spring relation shown as the dotted line) is elevated with respect to the reference (solid line, equation (1)). When mixing across the vortex edge is excluded (inset, shifted downward by 1.5 ppmv), the simulated spring relationship cannot be distinguished from the reference.

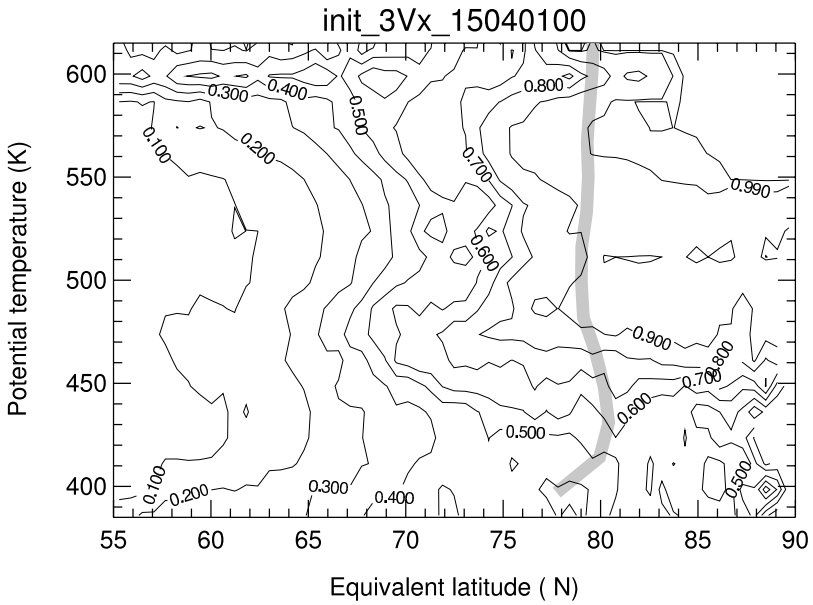

Figure 5. Contour plot of the vortex tracer (Tr_V) in ϕ_{eq}-θ space for April from the CLaMS simulation. The shading indicates the vortex boundary at $\phi_{eq} \approx 80°N$. The rather small vortex is the result of several warming pulses and persists until 16 April.

predicted from the reference correlation: The mean difference is +114 ppbv; this is the bias introduced on a chemically inactive ozone tracer by using a tracer-tracer correlation instead of O_3^{pass} for the simulated winter and translates to an ozone column loss underestimation of 6 DU (integrated between 380 and 550 K). This bias is independent of chemical ozone loss, as is demonstrated in equation (A3) in Appendix A.

[24] We confirmed this finding experimentally by introducing two pseudochemically active O_3 tracers O_3^{chem} and O_3^{chem*2}, both initialized with the original O_3 field at simulation start. Chemical ozone loss was imposed by daily subtraction of a loss profile averaging 10 ppbv d^{-1} for O_3^{chem} (20 ppbv d^{-1} for O_3^{chem*2}), corresponding to an expected final loss column of 37 DU (74 DU). An evaluation with TRAC after the simulation yields 31 DU (68 DU), which is an underestimation of ozone loss of 6 DU in both cases. At typical vortex-average losses of 1 ppmv or 60 DU over an Arctic winter, the underestimation, and thus the error of the TRAC technique, is on the order of 10%.

[25] Figure 4 demonstrates that the early winter reference relationship is closely matched by the spring CH_4-O_3^{pass} relationship only for data within the polar vortex. Data outside the vortex ($\phi_{eq} < 80°N$) cannot be represented well with the early winter correlation. It is critical for the TRAC method that only vortex data are considered: Including data from the outer edge of the vortex (e.g., $75°N < \phi_{eq} < 80°N$, green color in Figure 4) results in a large misrepresentation by the reference correlation.

[26] A passive tracer marking the interior of the initial vortex (Tr_V) quantifies dilution of vortex air due to mixing with midlatitude air (Figure 5). Above 450 K, the vortex edge coincides with the 90% isopleth of Tr_V: The vortex is well isolated. Toward midlatitudes the 50% isopleth is located at $\phi_{eq} \approx 70°N$ (corresponding to the extent of the January vortex). APs are composed of half vortex and half midlatitude air in this outer edge region, which is partly composed of remains of vortex air left behind when the vortex area decreases during stratospheric warming events. Below 450 K the vortex is unstable during the last week of the 90-day simulation period. Midlatitude air is brought to higher latitudes: The 50% isopleth coincides with the vortex edge at $\phi_{eq} = 80°N$. However, at these lower altitudes the slopes of the midlatitude and vortex relationships are rather similar, such that the error made by the TRAC analysis is minimized (see Appendix A). From the separation between vortex and midlatitude relationships (Figure 3) and the fraction of vortex air at the vortex edge (Figure 5) as a proxy for mixing intensity, the error introduced by the TRAC method (equation (A3)) can be calculated. The expected error lies in the range 10–160 ppbv and compares well with the CLaMS-simulated average bias of 114 ppbv.

[27] The winter-to-spring descent of a passive tracer of initial potential temperature (Tr_θ) is shown in Figure 6 for APs arriving within ±15 K around 475 K on 1 April. Strongest descent of about 100 K occurs around $\phi_{eq} = 60°N$, building up a gradient of more than 75 K differential descent toward the vortex center. Two thirds of this gradient are located within the polar vortex. The differential descent would impact the applicability of TRAC on the curved relationships between CH_4 and O_3, if it were subsequently followed by homogenization of the vortex through internal mixing. However, the presence of a large descent gradient (black line in Figure 6) within the vortex demonstrates that the vortex is not homogenized across equivalent latitudes.

[28] Assuming (unrealistically) the complete homogenization of the vortex air on one isentropic level, we can obtain an upper boundary to the effect of internal mixing. At minimum and maximum CH_4 mixing ratio 1.36 and 1.48 ppmv within the vortex at 475 K (obtained from the CLaMS simulation) O_3^{mixed} is −80 ppbv less than O_3^{ref}. As evident in the strong descent gradient in spring (Figure 6),

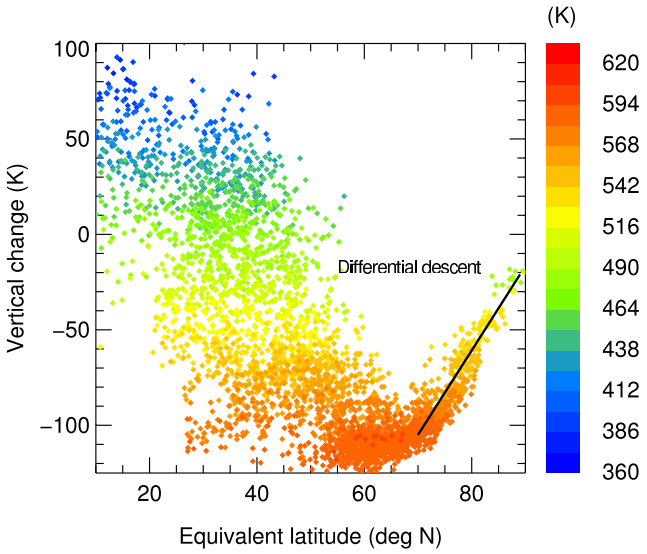

Figure 6. Vertical change of APs arriving at 475 K, derived from a CLaMS simulation with a passive tracer of potential temperature (Tr_θ). Color indicates the mean of each mixed AP's source altitudes. The large gradient from the vortex outer edge to the core indicates differential descent (black line): Air masses outside the vortex are composed of upper boundary air (red), core vortex air descended by about 25 K.

homogenization of the vortex did not follow differential descent. Rather, one can assume that differential descent and internal mixing occur throughout the winter between AP close to one another in tracer space [e.g., *Plumb and Ko*, 1992; *Plumb et al.*, 2000]. Such small and frequent steps of differential descent and internal mixing result in only minor deviations from the reference relation. In fact, differential descent followed by internal mixing is necessary for the compactization of early winter tracer-tracer relationships [*Ray et al.*, 2002].

[29] The above considerations demonstrate that internal mixing cannot be a large source of error when looking at TRAC-derived chemical O_3 loss in CLaMS. A quantification of internal mixing effects on chemical O_3 loss is demonstrated in the following, utilizing Lagrangian AP identities, the control over mixing in CLaMS, and the tracer Tr_V: The influence of APs that are mixed across the edge of the vortex is removed selectively (Figure 7), such as to isolate internal mixing effects on the CH_4-O_3 relationship. Cross-vortex processes, i.e., injection or mixing of midlatitude air into the vortex are evident in values of $Tr_V < 1$ within the vortex. For these APs (shown in red in Figure 7) the O_3 change due to cross vortex-boundary mixing is removed by assigning to these APs a new O_3 value based on the early vortex reference relation. Tr_V is subsequently reinitialized to one within the ϕ_{eq}-contour defined vortex and to zero otherwise. The now isolated effect of internal mixing is negligible (<10 ppbv), emphasizing that the largest error introduced by using TRAC comes from mixing across the vortex edge. Figure 4 (inset) illustrates that there is no visible difference between the spring tracer relation inside the vortex and the early winter reference relation when cross vortex boundary mixing is selectively excluded. Within the time slice, this coldest winter can be expected to exhibit the largest differential descent, and the largest impact of internal mixing on TRAC-derived O_3 loss. The fact that even under these circumstances TRAC is not noticeably affected suggests that TRAC on warmer winters with less differential descent is not severely affected, either.

5. From CTM to CCM

[30] With the above described experiments we calculated the deviation of a passive ozone tracer from the reference correlation in a Lagrangian CTM (on CCM winds) with tight control of mixing. We exploit this control over mixing to operate the CTM in a highly diffusive regime comparable to that of a CCM. Numerical diffusion in a model is expected to increase mixing; for example, *Reithmeier and Sausen* [2002] found a tenfold increase of the most stable radon isotope (^{222}Rn, $\tau_{1/2}$ = 3.8 days) gradient at 100 hPa in their Lagrangian transport scheme ATTILA compared to the semi-Lagrangian scheme by *Williamson and Rasch* [1994] in ECHAM4. In a study of the breakup phase of the Arctic polar vortex, *Piani et al.* [2002] found that the separation of the midlatitude and vortex relationship was larger in observations than in their model and attribute this difference to numerical diffusion.

[31] The study of probability density functions (PDFs) of tracer differences between air parcels separated by a pre-

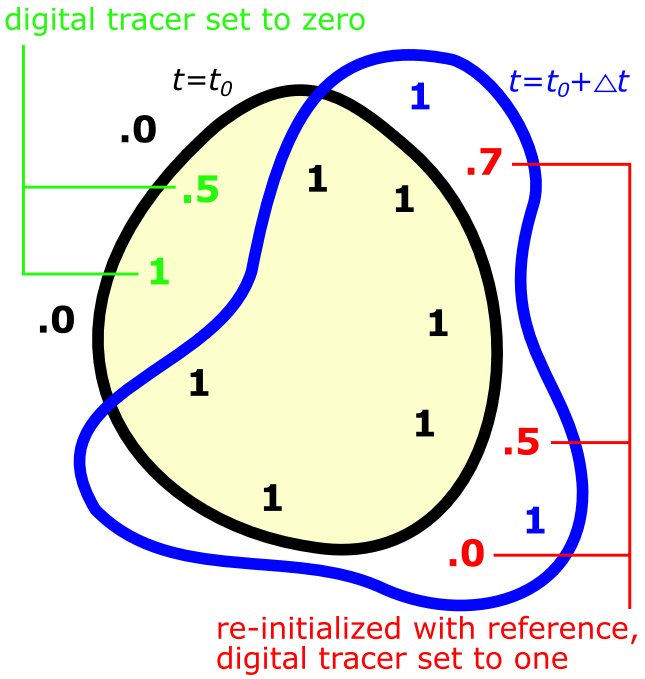

Figure 7. Schematic diagram of the strategy to eliminate cross-vortex mixing from a CLaMS simulation at every time step. On the basis of prior distribution of the vortex tracer Tr_V (black, $t = t_0$) all APs that were advected or mixed into a later vortex (blue solid contour, at $t = t_0 + \Delta t$) and therefore have $Tr_V < 1.0$ (red) are reinitialized with the vortex correlation. Tr_V is reinitialized to zero outside (green) and to one inside the vortex before the next time step.

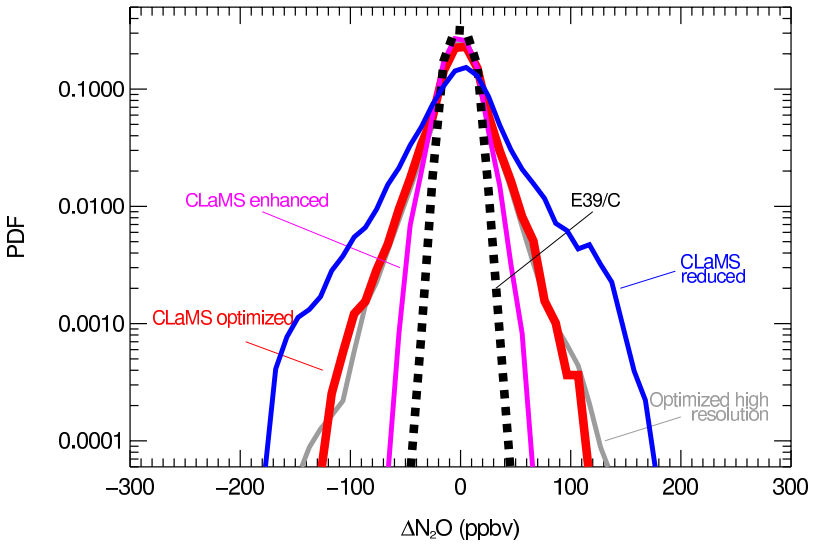

Figure 8. Probability density function of neighboring air parcel N_2O difference from CLaMS simulations (solid lines, increased mixing parameterization from broad to slim distribution) and E39/C (dotted line). Air parcel statistic confined to region north of 60°N and with AP distance <500 km.

scribed distance offers an effective way to analyze the variability of tracer distributions [e.g., *Sparling*, 2000; *Sparling and Bacmeister*, 2001]. In turbulent flows, an anomalously high probability of extreme spatial fluctuations of tracers, termed intermittency, is expected, and consequently, the corresponding PDFs are characterized by a Gaussian core and non-Gaussian "fat" tails [*Shraiman and Siggia*, 2000]. An important advantage of using this technique is that different models can be compared with respect to their ability to resolve the spatial variability of tracers even if the simulated structures do not perfectly match, e.g., due to inaccuracies in the advection scheme. Such errors cannot significantly change the statistics of the tracer differences and thus the shape of the PDFs.

[32] To compare E39/C with its semi-Lagrangian transport scheme [*Williamson and Rasch*, 1994] and associated high numerical diffusion to CLaMS results, we evaluate the PDFs of the N_2O mixing ratio gradient in both CLaMS simulations and E39/C data. A recent study by *Khosrawi et al.* [2005] made use of tracer difference PDFs in CLaMS to compare CLaMS results with satellite observations from the Cryogenic Infrared Spectrometer and Telescope for the Atmosphere (CRISTA [*Offermann et al.*, 1999]) instrument and to the Eulerian CTM Karlsruhe Simulation model of the Middle Atmosphere (KASIMA [*Kouker et al.*, 1999]). KASIMA in turn was used by *Eyring et al.* [2003] for the validation of E39/C subtropical mixing.

[33] Figure 8 shows the PDF of N_2O differences on 1 April from the E39/C tracer field (dotted line) and CLaMS simulations with optimized mixing (i.e., the reference setup used in this study, thick solid line), enhanced mixing (grid resolution r = 250 km, ℓ_c = 0.4 d^{-1}), and reduced mixing (r = 200 km, ℓ_c = 2.0 d^{-1}). Referring to *Khosrawi et al.* [2005], Figure 8 the reference simulation shows good agreement with CRISTA observations and the E39/C distribution is similar to KASIMA (note that their study uses different latitude range and time period). With the control over mixing that is possible in CLaMS, the diffusivity was continuously increased (lower resolution, shorter time interval, increasing Lyapunov exponent) to study the sensitivity of the tracer gradient PDF and vortex passive ozone to varying diffusion. The time interval is constrained by the availability of meteorological fields (shortest interval Δt = 12 hours) and the resolution by the stability of the three-dimensional air parcel distribution ($r \leq 300$ km, θ = 360–610 K). The PDF for enhanced mixing is shown in Figure 8 as the innermost solid line; overly enhanced mixing in CLaMS falls slightly short of simulating a distribution that matches the PDF generated from the E39/C April N_2O field.

[34] By imitating the E39/C tracer difference PDF with a CLaMS simulation, we show that the result of numerical diffusion is very similar in E39/C and CLaMS with enhanced mixing. We use this similarity of diffusion and the knowledge that both models use the same meteorological information to relate information on the TRAC technique gathered with CLaMS to E39/C. By analogy, we expect that TRAC applies to E39/C in the same manner as to CLaMS (enhanced mixing) and that the error estimate given for the TRAC method with CLaMS is of similar magnitude in E39/C. Table 1 summarizes the sensitivity of the TRAC error with respect to a passive ozone tracer for a

Table 1. Sensitivity of the Difference Between TRAC-Derived Chemical Column O_3 Loss and O_3 Loss Calculated With a Passive O_3 Tracer to Varying Diffusivity[a]

	r, km	ℓ_c	Δt hours	$\Delta O_3^{pass} - \Delta O_3^{ref}$ DU
Reduced	100	0.8	24	4.7
Reduced	200	2.0	24	5.9
Standard	200	1.2	24	5.9
Enhanced	200	0.2	24	7.7
Enhanced	250	0.6	24	5.1
Enhanced	250	0.4	24	8.3

[a]Results from selected CLaMS simulations are shown.

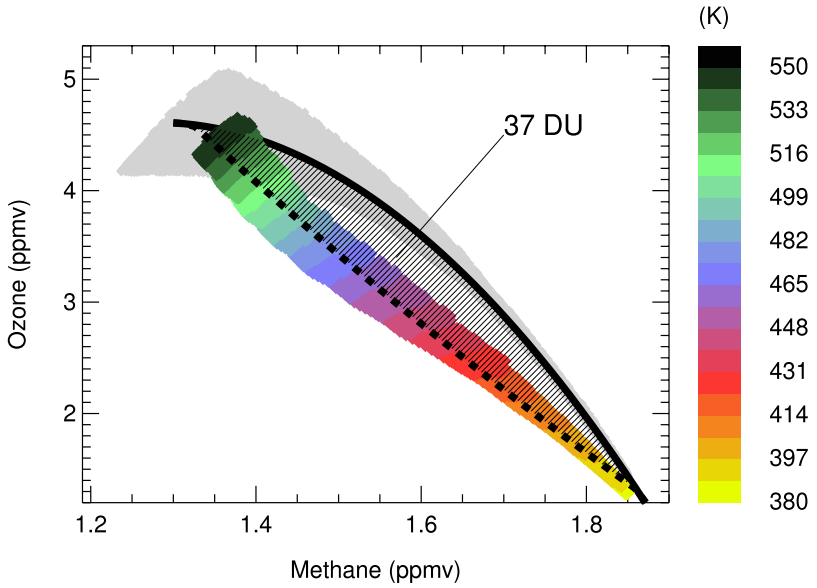

Figure 9. E39/C methane-ozone vortex correlation for January (grey) and April (colored, color indicates potential temperature). Chemical column ozone loss (hatched area) is evaluated between the polynomial fits to both correlations and amounts to 37 DU.

range of CLaMS simulations with different mixing intensity. The largest TRAC overestimation was found for the CLaMS simulation with most enhanced mixing, though no significant trend could be determined. Overestimates range from 4.7 to 8.3 DU; the TRAC error on E39/C wind field due to mixing should be similar to the latter value, found for large CLaMS diffusivity.

[35] Using the tracer-tracer correlation technique, the 90-day chemical ozone loss calculated for the coldest winter of the '2015' time slice is 37 DU, integrated between 380 and 550 K potential temperature (Figure 9). To compare this value to chemical ozone loss calculated for winters of the 1990s several effects have to be considered: (1) the underestimation introduced by the TRAC method, (2) the lower chlorine loading (−9%) specified for 2015 versus 1990, and (3) absence of bromine cycles in E39/C; bromine reactions may be responsible for at least 25% [*Bregman et al.*, 1997] and up to 50% [*Frieler et al.*, 2006] of chemical ozone loss. If we assume that bromine cycles are roughly responsible for one third of the chemical loss, we need to add 50% to the results from a simulation without Br; if chemical ozone loss decreases to a first order approximation linear with chlorine loading, we need to add 11% to scale from 2015 to 1990 boundary conditions; finally we add 8.3 DU to correct for the TRAC underestimation. To compare the E39/C TRAC-calculated chemical ozone loss of 37 DU in 2015 to the 1990s, the term 37 DU × 150% × 111% + 8.3 DU yields a value of 70 DU.

[36] This hypothetical value for the 1990s compares well to observed cold Arctic winter chemical ozone loss: *Harris et al.* [2002] show for the cold Arctic winter 1999/2000 chemical ozone loss on the order of 80–105 DU across a variety of methods. *Rex et al.* [2004] calculate between 57 and 103 DU for the coldest winters (1992/1993, 1994/1995, 1995/1996, 1996/1997, 1999/2000) of the 1990s; for these winters, *Tilmes et al.* [2004] give a range of 46–92 DU.

6. Conclusion

[37] The principle action of internal mixing and mixing across the vortex edge on ozone loss derived with the tracer-tracer correlation technique (TRAC) is discussed in detail. Compared to both a reference relation and to a starting value, the ozone decrease in internally mixed air parcels may in principle be falsely interpreted as being due to photochemical ozone destruction. However, it is unlikely that the required homogenization within the vortex only occurs after a period of unmixed differential descent. If differential descent and internal mixing occur in frequent small steps, the error introduced into chemical ozone loss estimates is small.

[38] Mixing-in of midlatitude O_3-rich air increases O_3 relative to CH_4, can mask chemical ozone loss and lead to an underestimation of chemical ozone loss when calculated with TRAC. This underestimation is consistent across all altitudes where chemical ozone loss occurs and is independent of the shape of isentropes in tracer-tracer space. Techniques that calculate chemical ozone loss with respect to an earlier ozone observation may underestimate or overestimate chemical loss depending on the shape of isentropes. The error in the determination of TRAC-derived chemical ozone loss decreases with decreasing altitude. Thus TRAC minimizes the error of column chemical ozone loss calculations where the largest contribution to the O_3 column comes from lower altitudes.

[39] We assess the applicability of the tracer-tracer correlation method as a tool for deducing ozone loss from the results of chemistry-climate models. Two requirements for successful application of TRAC have to be met: (1) existence of a compact early winter vortex relationship and

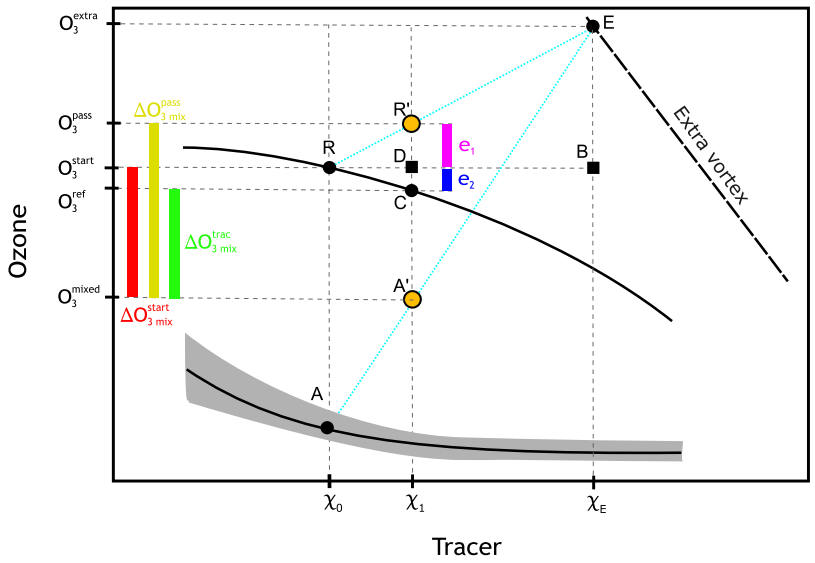

Figure A1. Sketch of the impact of mixing on ozone loss calculations which use either a reference (O_3^{ref}) or an initial ozone value (O_3^{start}) or passive ozone (O_3^{pass}). The difference between each of the three methods depends on (1) mixing intensity, (2) the slope of the reference relation (solid curve), and (3) the separation of vortex and midlatitude (dashed line) relationships, given by the length of the line segments [BE] and [RB]. Differences between the three techniques are independent of chemical ozone loss $\overline{AR}$.

(2) sufficient isolation of the vortex over the winter/spring episode. For modeled data only, the additional influence of numerical diffusion on TRAC has to be quantified. For the E39/C simulation, we confirm that the necessary requirements are fulfilled. We employ the chemistry transport model CLaMS to independently provide a measure of spring ozone from a passive ozone tracer (O_3^{pass}) and evaluate the performance of TRAC. In high-diffusivity CLaMS experiments we show by analogy that enhanced numerical diffusion has only a small effect on TRAC-derived chemical O_3 loss in E39/C.

[40] With respect to the passive ozone method, TRAC underestimated chemical ozone loss by 4–8 DU due to mixing processes and numerical diffusion; at the typical magnitude of Arctic ozone loss, the relative error is ~10%. We quantify separately the effects of internal mixing and mixing across the vortex boundary on TRAC-derived chemical ozone loss: The underestimation of ozone loss by TRAC is found to be dominated by mixing across the vortex boundary. A technique to isolate internal mixing from mixing across the vortex edge in a Lagrangian transport model is provided. Internal mixing does not impact the analysis of ozone loss by the TRAC technique even for the case of strong differential descent.

[41] This first successful application of TRAC on a CCM simulation is an important milestone: chemical ozone loss from a variety of CCMs can be calculated with TRAC if the necessary TRAC requirements are met and if the magnitude of additional mixing introduced by numerical diffusion on TRAC can be estimated. The error for a particular CCM can be assessed by comparing passively transported ozone from a chemistry transport model simulation to TRAC-derived ozone. Since the validation of CCMs has recently been brought forward by a SPARC initiative [*Eyring et al.*, 2005], we propose that within this framework, CTMs such as CLaMS should be routinely applied for the validation of chemical ozone loss in CCMs.

[42] There is a large and yet unused potential of TRAC to analyze existing CCM results for chemically destroyed ozone. With TRAC, it will be possible to extract information about chemical ozone loss from archived CCM simulations, which would otherwise have required expensive new simulations with these CCMs. With this new information about chemical ozone loss from existing climate model simulations, we should be able to make improved predictions of past and future simulated halogen impact.

[43] We conclude that the tracer-tracer correlation technique (TRAC) is a conservative and consistent measure of chemical ozone loss. Its area of application is not limited to observations but should be expanded to simulated data as well.

Appendix A: Bias of TRAC Under Chemical O_3 Loss

[44] Intuitively, the effect of mixing across the vortex on O_3 loss estimates depends on the magnitude of chemical ozone loss: the larger the separation between the midlatitude relationship and a relationship inside the vortex is, the more does mixing affect the loss calculation. However, we demonstrate here that the difference between three widely used methods to determine chemical ozone loss does not depend on the magnitude of chemical ozone loss. Let us suppose that chemical ozone loss occurred in an air parcel represented as point A in Figure A1, which lies below point R on the reference relation; R also represents the value of a passive ozone tracer. After a mixing event across the vortex with an air parcel E, A, and R are mixed along mixing lines to A′ and R′. The intensity of mixing is given by $(1 - \beta) = \overline{RR'}/\overline{RE}$ where β is the fraction of vortex air after a mixing

event and $\beta = 1$ corresponds to no mixing. With the passive ozone tracer method, ozone loss equals

$$\Delta O_3^{pass} = \overline{A'R'} = \beta\overline{AR}. \quad (A1)$$

Mixing decreases the initial ozone loss $\overline{AR}$ to $\overline{A'R'}$; the difference between $\overline{A'R'}$ and $\overline{AR}$ is proportional to chemical ozone loss and to mixing intensity.

[45] If one evaluates chemical ozone loss against a fixed starting value of ozone the calculated chemical loss becomes

$$\begin{aligned}\Delta O_3^{start}\overline{A'D} &= \overline{A'R'} - \overline{DR'} \\ &= \Delta O_3^{pass} - (1-\beta)\overline{BE}. \end{aligned} \quad (A2)$$

The error $e_1 = \overline{DR'}$ of this method with respect to the passive ozone tracer is proportional to mixing intensity and proportional to the vertical separation of midlatitude and reference relations $\overline{BE}$. Depending on the relative position of B and E, ozone loss can be overestimated or underestimated.

[46] Chemical ozone loss evaluated with TRAC deviates from ΔO_3^{pass} by $e_1 + e_2 = \overline{CD'}$. The summand $e_2 = \overline{CD}$ can be calculated from the slope of the reference relation $\gamma = -\overline{CD}/\overline{RD}$ and the horizontal component of the separation between midlatitude and reference relation $\overline{RB}$.

$$\begin{aligned}\Delta O_3^{trac} &= \overline{A'C} = \overline{A'R'} - \overline{CD} - \overline{DR'} \\ &= \Delta O_3^{pass} - \gamma\overline{RD} - (1-\beta)\overline{BE} \\ &= \Delta O_3^{pass} - (1-\beta)\gamma\overline{RB} - (1-\beta)\overline{BE}, \end{aligned} \quad (A3)$$

The TRAC error $e_1 + e_2$ is proportional to mixing intensity and increases with the separation of vortex and midlatitude relationships; it is independent of chemical ozone loss $\overline{AR}$. Even for negative values of e_1 the sum $e_1 + e_2$ is positive, because the magnitude of the slope of the vortex relationship is greater than the slope of any isentrope and thus $e_2 > -e_1$; when the vortex slope is close to the slope of the midlatitude relationship, the TRAC error is at its minimum: TRAC consistently underestimates chemical ozone loss compared to a passive ozone tracer.

[47] **Acknowledgments.** The work presented here was partly funded by the German National Research Program AFO2000, project KODYACS/LAVERO (FKZ 07ATF43). Much of the E39/C data preprocessing was kindly handled by F. Mager of DLR Oberpfaffenhofen. We are grateful to K. Shine, J. Haigh and W. Zhong for providing the radiation code. We received helpful comments on the manuscript from M. Rex and two anonymous referees. We thank M. von Hobe, S. Rohs, G. Günther, J. Grooß and the CLaMS development team at ICG-I for discussions and technical support.

References

Austin, J. (2002), A three-dimensional coupled chemistry-climate model simulation of past stratospheric trends, *J. Atmos. Sci.*, *59*(2), 218–232.

Austin, J., et al. (2003), Uncertainties and assessments of chemistry-climate models of the stratosphere, *Atmos. Chem. Phys.*, *3*, 1–27, sref:1680-7324/acp/2003-3-1.

Bregman, A., M. van den Broek, K. S. Carslaw, R. Müller, T. Peter, M. P. Scheele, and J. Lelieveld (1997), Ozone depletion in the late winter lower Arctic stratosphere: Observations and model results, *J. Geophys. Res.*, *102*, 10,815–10,828.

de Grandpré, J., S. R. Beagley, V. I. Fomichev, E. Griffioen, J. C. McConnell, A. S. Medvedev, and T. G. Shepherd (2000), Ozone climatology using interactive chemistry: Results from the Canadian Middle Atmosphere Model, *J. Geophys. Res.*, *105*, 26,475–26,492.

Esler, J. G., and D. W. Waugh (2002), A method for estimating the extent of denitrification of Arctic polar vortex air from tracer-tracer scatter plots, *J. Geophys. Res.*, *107*(D13), 4169, doi:10.1029/2001JD001071.

Eyring, V., M. Dameris, V. Grewe, I. Lanbein, and W. Kouker (2003), Climatologies of subtropical mixing derived from 3D models, *Atmos. Chem. Phys.*, *3*, 1007–1021, sref:1680-7324/acp/2003-3-1007.

Eyring, V., et al. (2005), A strategy for process-oriented validation of coupled chemistry-climate models, *Bull. Am. Meteorol. Soc.*, *86*(8), 1117–1133.

Fahey, D. W., K. K. Kelly, G. V. Ferry, L. R. Poole, J. C. Wilson, D. M. Murphy, M. Loewenstein, and K. R. Chan (1989), In situ measurements of total reactive nitrogen, total water, and aerosol in a polar stratospheric cloud in the Antarctic, *J. Geophys. Res.*, *94*, 11,299–11,315.

Fairlie, T. D., R. B. Pierce, J. A. Al-Saadi, W. L. Grose, J. M. Russell, M. H. Proffitt, and C. R. Webster (1999), The contribution of mixing in Lagrangian photochemical predictions of polar ozone loss over the Arctic in summer 1997, *J. Geophys. Res.*, *104*, 26,597–26,609.

Frieler, K., M. Rex, R. J. Salawitch, T. Canty, M. Streibel, R. M. Stimpfle, K. Pfeilsticker, M. Dorf, D. K. Weisenstein, and S. Godin-Beekmann (2006), Toward a better quantitative understanding of polar stratospheric ozone loss, *Geophys. Res. Lett.*, *33*, L10812, doi:10.1029/2005GL025466.

Goutail, F., et al. (2005), Early unusual ozone loss during the Arctic winter 2002/2003 compared to other winters, *Atmos. Chem. Phys.*, *5*, 665–677.

Hanson, D. R., and K. Mauersberger (1988), Laboratory studies of the nitric acid trihydrate: Implications for the south polar stratosphere, *Geophys. Res. Lett.*, *15*(8), 855–858.

Harris, N. R., M. Rex, F. Goutail, B. M. Knudsen, G. L. Manney, R. Müller, and P. von der Gathen (2002), Comparison of empirically derived ozone loss rates in the Arctic vortex, *J. Geophys. Res.*, *107*(D20), 8264, doi:10.1029/2001JD000482.

Hein, R., et al. (2001), Results of an interactively coupled atmospheric chemistry-general circulation model: Comparison with observations, *Ann. Geophys.*, *19*, 435–457, sref:1432-0576/ag/2001-19-435.

Intergovernmental Panel on Climate Change/Technology and Economic Assessment Panel (2005), *Special Report on Safeguarding the Ozone Layer and the Global Climate System: Issues Related to Hydrofluorocarbons and Perfluorocarbons*, edited by B. Metz et al., 488 pp., Cambridge Univ. Press, New York.

Khosrawi, F., J.-U. Grooß, R. Müller, P. Konopka, W. Kouker, R. Ruhnke, T. Reddmann, and M. Riese (2005), Intercomparison between Lagrangian and Eulerian simulation of the development of mid-latitude streamers as observed by CRISTA, *Atmos. Chem. Phys.*, *5*, 85–95, sref:1680-7324/acp/2005-5-85.

Knudsen, B. M., et al. (1998), Ozone depletion in and below the Arctic vortex for 1997, *Geophys. Res. Lett.*, *25*(5), 627–630.

Konopka, P., et al. (2004), Mixing and ozone loss in the 1999–2000 Arctic vortex: Simulations with the 3-dimensional Chemical Lagrangian Model of the Stratosphere (CLaMS), *J. Geophys. Res.*, *109*, D02315, doi:10.1029/2003JD003792.

Konopka, P., J.-U. Grooß, K. Hoppel, H.-M. Steinhorst, and R. Müller (2005), Mixing and chemical ozone loss during and after the Antarctic polar vortex major warming in September 2002, *J. Atmos. Sci.*, *62*(3), 848–859.

Kouker, W., D. Offermann, V. Küll, T. Reddmann, R. Ruhnke, and A. Franzen (1999), Streamers observed by the CRISTA experiment and simulated in the KASIMA model, *J. Geophys. Res.*, *104*, 16,405–16,418.

Labitzke, K. (1999), *Die Stratosphäre: Geschichte, Phänomene, Relevanz*, 174 pp., Springer, New York.

Land, C., J. Feichter, and R. Sausen (2002), Impact of vertical resolution on the transport of passive tracers in the ECHAM4 model, *Tellus, Ser. B*, *54*(4), 344–360, doi:10.1034/j.1600-0889.2002.201367.x.

Lefèvre, F., F. Figarol, K. S. Carslaw, and T. Peter (1998), The 1997 Arctic ozone depletion quantified from three-dimensional model simulations, *Geophys. Res. Lett.*, *25*, 2425–2428.

Manney, G. L., L. Froidevaux, M. L. Santee, R. W. Zurek, and J. W. Waters (1997), MLS observations of Arctic ozone loss in 1996–97, *Geophys. Res. Lett.*, *24*(22), 2697–2700.

McKenna, D. S., J.-U. Grooß, G. Günther, P. Konopka, R. Müller, G. Carver, and Y. Sasano (2002a), A new Chemical Lagrangian Model of the Stratosphere (CLaMS): 2. Formulation of chemistry scheme and initialization, *J. Geophys. Res.*, *107*(D15), 4256, doi:10.1029/2000JD000113.

McKenna, D. S., P. Konopka, J.-U. Grooß, G. Günther, R. Müller, R. Spang, D. Offermann, and Y. Orsolini (2002b), A new Chemical Lagrangian Model of the Stratosphere (CLaMS): 1. Formulation of advection and mixing, *J. Geophys. Res.*, *107*(D16), 4309, doi:10.1029/2000JD000114.

Michelsen, H. A., G. L. Manney, M. R. Gunson, and R. Zander (1998), Correlations of stratospheric abundances of NO_y, O_3, N_2O, and CH_4 derived from ATMOS measurements, *J. Geophys. Res.*, *103*, 28,347–28,359.

Morgenstern, O., A. M. Lee, and J. A. Pyle (2003), Cumulative mixing inferred from stratospheric tracer relationships, *J. Geophys. Res.*, *108*(D5), 8321, doi:10.1029/2002JD002098.

Müller, R., P. J. Crutzen, J.-U. Grooß, C. Brühl, J. M. Russel III, and A. F. Tuck (1996), Chlorine activation and ozone depletion in the Arctic vortex: Observations by the Halogen Occultation Experiment on the Upper Atmosphere Research Satellite, *J. Geophys. Res.*, *101*, 12,531–12,554.

Müller, R., P. J. Crutzen, J. U. Grooß, C. Brühl, J. M. Russel III, H. Gernandt, D. S. McKenna, and A. F. Tuck (1997), Severe chemical ozone loss in the Arctic during the winter of 1995–96, *Nature*, *389*, 709–712.

Müller, R., U. Schmidt, A. Engel, D. S. McKenna, and M. H. Proffitt (2001), The O_3/N_2O relationship from balloon-borne observations as a measure of Arctic ozone loss in 1991–1992, *Q. J. R. Meteorol. Soc.*, *127*, 1389–1412.

Müller, R., S. Tilmes, P. Konopka, J.-U. Grooß, and H.-J. Jost (2005), Impact of mixing and chemical change on ozone-tracer relations in the polar vortex, *Atmos. Chem. Phys.*, *5*, 3139–3151, sref:1680-7324/acp/2005-5-3139.

Nagashima, T., M. Takahashi, M. Takigawa, and H. Akiyoshi (2002), Future development of the ozone layer calculated by a general circulation model with fully interactive chemistry, *Geophys. Res. Lett.*, *29*(8), 1162, doi:10.1029/2001GL014026.

Nash, E. R., P. A. Newman, J. E. Rosenfield, and M. R. Schoeberl (1996), An objective determination of the polar vortex using Ertel's potential vorticity, *J. Geophys. Res.*, *101*, 9471–9478.

Offermann, D., K.-U. Grossmann, P. Barthol, P. Knieling, M. Riese, and R. Trant (1999), Cryogenic Infrared Spectrometers and Telescopes for the Atmosphere (CRISTA) experiment and middle atmosphere variability, *J. Geophys. Res.*, *104*, 16,311–16,325.

Piani, C., W. A. Norton, A. M. Iwi, E. A. Ray, and J. W. Elkins (2002), Transport of ozone-depleted air on the breakup of the stratospheric polar vortex in spring/summer 2000, *J. Geophys. Res.*, *107*(D20), 8270, doi:10.1029/2001JD000488.

Plumb, R. A., and M. K. W. Ko (1992), Interrelationships between mixing ratios of long-lived stratospheric constituents, *J. Geophys. Res.*, *97*, 10,145–10,156.

Plumb, R. A., D. W. Waugh, and M. P. Chipperfield (2000), The effect of mixing on tracer relationships in the polar vortices, *J. Geophys. Res.*, *105*, 10,047–10,062.

Proffitt, M. H., J. J. Margitan, K. K. Kelly, M. Loewenstein, J. R. Podolske, and K. R. Chan (1990), Ozone loss in the Arctic polar vortex inferred from high altitude aircraft measurements, *Nature*, *347*, 31–36.

Proffitt, M. H., S. Solomon, and M. Loewenstein (1992), Comparison of 2-D model simulations of ozone and nitrous oxide at high latitudes with stratospheric measurements, *J. Geophys. Res.*, *97*, 939–944.

Ray, E. A., F. L. Moore, J. W. Elkins, D. F. Hurst, P. A. Romashkin, G. S. Dutton, and D. W. Fahey (2002), Descent and mixing in the 1999–2000 northern polar vortex inferred from in situ tracer measurements, *J. Geophys. Res.*, *107*(D20), 8285, doi:10.1029/2001JD000961.

Reithmeier, C., and R. Sausen (2002), ATTILA – Atmospheric Tracer Transport In a LAgrangian model, *Tellus, Ser. B*, *54*(3), 278–299, doi:10.1034/j.1600-0889.2002.01236.x.

Rex, M., et al. (1999), Subsidence, mixing and denitrification of Arctic polar vortex air measured during POLARIS, *J. Geophys. Res.*, *104*, 26,611–26,623.

Rex, M., et al. (2002), Chemical depletion of Arctic ozone in winter 1999/2000, *J. Geophys. Res.*, *107*(D20), 8276, doi:10.1029/2001JD000533.

Rex, M., R. J. Salawitch, P. von der Gathen, N. R. Harris, M. P. Chipperfield, and B. Naujokat (2004), Arctic ozone loss and climate change, *Geophys. Res. Lett.*, *31*, L04116, doi:10.1029/2003GL018844.

Richard, E. C., et al. (2001), Severe chemical ozone loss in the Arctic polar vortex during winter 1999–2000 inferred from in-situ airborne measurements, *Geophys. Res. Lett.*, *28*(11), 2197–2200.

Roach, W. T. (1962), Aircraft observations in the lower sub-Arctic stratosphere in winter, *Meteorol. Res. Comm. Pap. 121*, Natl. Meteorol. Libr., Meteorol. Off., Bracknell, UK.

Salawitch, R. J., et al. (2002), Chemical loss of ozone during the Arctic winter of 1999–2000: An analysis based on balloon-borne observations, *J. Geophys. Res.*, *107*(D20), 8269, doi:10.1029/2001JD000620.

Sankey, D., and T. G. Shepherd (2003), Correlations of long-lived chemical species in a middle atmosphere general circulation model, *J. Geophys. Res.*, *108*(D16), 4494, doi:10.1029/2002JD002799.

Schnadt, C. (2001), Untersuchung der zeitlichen Entwicklung der stratosphärischen Chemie mit einem interaktiv gekoppelten Klima-Chemie-Modell, dissertation, Univ. ät München, Inst. für Phys. der Atmos. des Dtsch. Zentrum fr Luft- und Raumfahrt, Oberpfaffenhofen, Germany.

Schnadt, C., and M. Dameris (2003), Relationship between North Atlantic Oscillation changes and stratospheric ozone recovery in the Northern Hemisphere in a chemistry-climate model, *Geophys. Res. Lett.*, *30*(9), 1487, doi:10.1029/2003GL017006.

Schnadt, C., M. Dameris, M. Ponater, R. Hein, V. Grewe, and B. Steil (2002), Interaction of atmospheric chemistry and climate and its impact on stratospheric ozone, *Clim. Dyn.*, *18*, 501–517.

Shraiman, B., and E. D. Siggia (2000), Scalar turbulence, *Nature*, *405*, 639–646.

Sinnhuber, B.-M., et al. (2000), Large loss of total ozone during the Arctic winter of 1999/2000, *Geophys. Res. Lett.*, *27*, 3473–3476.

Sparling, L. C. (2000), Statistical perspectives on stratospheric transport, *Rev. Geophys.*, *38*(4), 417–436.

Sparling, L. C., and J. T. Bacmeister (2001), Scale dependence of tracer microstructure: PDFs, intermittency and the dissipation scale, *Geophys. Res. Lett.*, *28*(14), 2823–2826.

Steil, B., M. Dameris, C. Brühl, P. J. Crutzen, V. Grewe, M. Ponater, and R. Sausen (1998), Development of a chemistry module for GCMs: First results of a multiannual integration, *Ann. Geophys.*, *16*, 205–228, sref:1432-0576/ag/1998-16-205.

Steil, B., C. Brühl, E. Manzini, P. J. Crutzen, J. Lelieveld, P. J. Rasch, E. Roeckner, and K. Krüger (2003), A new interactive chemistry-climate model: 1. Present-day climatology and interannual variability of the middle atmosphere using the model and 9 years of HALOE/UARS data, *J. Geophys. Res.*, *108*(D9), 4290, doi:10.1029/2002JD002971.

Steinhorst, H.-M., P. Konopka, G. Günther, and R. Müller (2005), How permeable is the edge of the Arctic vortex—Model studies of the winter 1999–2000, *J. Geophys. Res.*, *110*, D06105, doi:10.1029/2004JD005268.

Tilmes, S., R. Müller, J.-U. Grooß, and J. M. Russell (2004), Ozone loss and chlorine activation in the Arctic winters 1991–2003 derived with the tracer-tracer correlations, *Atmos. Chem. Phys.*, *4*(8), 2181–2213, sref:1680-7324/acp/2004-4-2181.

Tilmes, S., R. Müller, J. Grooß, R. Spang, T. Sugita, H. Nakajima, and Y. Sasano (2006), Chemical ozone loss and related processes in the Antarctic winter 2003 based on Improved Limb Atmospheric Spectrometer (ILAS)-II observations, *J. Geophys. Res.*, *111*, D11S12, doi:10.1029/2005JD006260.

Ulanovskii, A. E., A. N. Luk'yanov, V. A. Yushkov, N. M. Sitnikov, M. Volk, E. V. Ivanova, and F. Ravegnani (2004), Estimation of the chemical loss of ozone in the Antarctic stratosphere in the 1999 winter-spring season from direct measurements and simulations, *Izv. Russ. Acad. Sci. Atmos. Oceanic Phys., Engl. Transl.*, *40*(6), 695–703.

von der Gathen, P., et al. (1995), Observational evidence for chemical ozone depletion over the Arctic in winter 1991–92, *Nature*, *375*, 131–134, doi:10.1023/A:1010607521870.

Williamson, D. L., and P. J. Rasch (1994), Water vapour transport in the NCAR CCM2, *Tellus, Ser. A*, *46*, 34–51.

World Meteorological Organization (WMO) (1999), Scientific assessment of ozone depletion: 1998, *Rep. 44*, Geneva, Switzerland.

World Meteorological Organization (WMO) (2003), Scientific assessment of ozone depletion: 2002, *Rep. 47*, Geneva, Switzerland.

Zhong, W., and J. D. Haigh (1995), Improved broadband emissivity parameterization for water vapor cooling rate calculations, *J. Atmos. Sci.*, *52*(1), 124–138.

M. Dameris, Institut für Physik der Atmosphäre, Deutsches Zentrum für Luft- und Raumfahrt e.V., Oberpfaffenhofen, D-82234 Wessling, Germany.

P. Konopka and R. Müller, Institut für Chemie und Dynamik der Geosphäre I: Stratosphäre, Forschungszentrum Jülich GmbH, D-52425 Jülich, Germany.

C. Lemmen, Copernicus Instituut voor Duurzame Ontwikkeling en Innovatie, Sectie Natuurwetenschappen en Samenleving (NW&S), Universiteit Utrecht, Heidelberglaan 2, NL-3584 CS Utrecht, Netherlands. (c.lemmen@fz-juelich.de)